Fully distributed real-time voltage control in active distribution networks with large penetration of solar inverters

Antonin Colot[a,b]
Dpt. of Elec. Eng. and Comp. Sc.
University of Liège
Liège, Belgium
antonin.colot@uliege.be

Thomas Stegen[a]
Dpt. of Elec. Eng. and Comp. Sc.
University of Liège
Liège, Belgium
tstegen@uliege.be

Bertrand Cornélusse
Dpt. of Elec. Eng. and Comp. Sc.
University of Liège
Liège, Belgium
bertrand.cornelusse@uliege.be

***Abstract*—This work addresses voltage regulation problems in low-voltage distribution networks with a large penetration of solar photovoltaic inverters. We propose a fully distributed algorithm that computes solar inverters' active and reactive power setpoints. We consider a convex surrogate of the Branch Flow Model, which is solved iteratively using the Alternating Direction Method of Multipliers (ADMM). Improved voltage regulation is achieved by using local voltage measurements. Only active power curtailment and inverter losses are minimized to maximize the inverter owner's profit. The algorithm is tested on low-voltage (LV) networks with more than 100 buses. This method outperforms a currently implemented scheme in LV networks while showing results close to perfect centralized control.**

***Index Terms*—active distribution networks, volt-var control, volt-watt control, distributed algorithms**

I. Introduction

In recent years, there has been an increase in the number of photovoltaic (PV) installations for domestic usage, which has impacted low-voltage (LV) distribution networks. This results from rising energy costs, declining PV prices, suitability of PV for household use, and a variety of government incentives designed to encourage the use of renewable energies [1]. Historically, LV networks were designed for unidirectional power flows. High penetration of PV systems can reverse these flows, leading to overvoltage problems [2], [3], which can, in turn, cause disconnection of PV systems and reduction in the lifespan of electrical appliances in households [1]. Furthermore, this restricts the maximum number of PV installations supported by the distribution network [4].

Traditional techniques use on-load tap changers (OLTC), switched capacitors, or static voltage regulators (SVC) to mitigate voltage issues in LV networks [3]. They have been used for a while but were not designed to handle fast varying distributed energy resources [5], [6]. A frequent operation of these devices can shorten their life expectancy [1]. New control strategies have been encouraged because of the failure of traditional techniques to address overvoltage efficiently. The development of communication technology and the flexibility of power electronics converters opened the door for new voltage regulation methods in LV networks. The different control schemes can be classified based on their communication infrastructure [7].

When the control is centralized, a controller gathers the measurements throughout the complete electrical network, computes optimal power setpoints, and disseminates them to all the distributed units. This requires a complex communication infrastructure prone to failures and significant delays. Therefore, modern methods usually rely on two-level control strategies rather than just a centralized optimization problem for the real-time operation of LV networks.

In [5], local Q-V and P-V curves are computed based on forecasts for the next scheduled day and delivered back to PV systems. This hybrid control scheme is also considered in [8], where the Q-V curves are computed based on the measurements given by several distributed generators (DGs). In [9], the operator computes a day-ahead dispatch plan, and a distributed model predictive control is responsible for tracking this plan in real-time.

Centralized controllers ensure optimality. However, they are vulnerable to cyberattacks and data privacy issues. A fully decentralized controller could protect data privacy because it would not require communication. In [10], the authors have exploited historical data to compute optimal setpoints using an offline chance-constrained optimization problem. Local controllers are then tuned using machine-learning techniques based on the calculated setpoints. In [6], deep convolutional networks are fitted on optimal setpoints calculated from historical data to create 3-dimensional optimal local control curves. In [11], a reactive and active power regulation based on droop control is derived using a short-term PV prediction to forecast overvoltages.

Decentralized control is quick and well-suited for LV networks in real-time, but it results in suboptimal operation. Distributed algorithms are a trade-off between centralized and decentralized control strategies. They only need reduced

[a] Authors with equal contributions
[b] Colot Antonin is a Research Fellow of the Fonds de la Recherche Scientifique - FNRS

communication to take decisions locally. They are well suited to address overvoltage issues in LV networks because they aim for global optimality using disseminated controllers and minimal communication burden. Additionally, they can ensure data privacy and improve robustness against cyber-attacks or communication failure. In [12] and [13], authors use the dual-ascent method to solve an optimization problem distributed over each electrical node. After updating the Lagrangian multipliers, they are exchanged among neighbors through a communication network. In [14], authors also employ the dual-ascent method, but they exchange Lagrangian multipliers to equalize the angle differences across a line from both ends.

In [15], authors show that ADMM has superior convergence properties to the dual-ascent method. They consider the consensus-based version of ADMM and assume that the active power flows along the lines can be measured. In [16], the problem is split into several zones consisting of several electrical nodes, and a consensus-based ADMM is implemented. They use a quasi-Newton approach for the dual update to further enhance convergence properties. A convex surrogate of a distributed AC-OPF problem is solved using ADMM in [17]. The centralizer computes voltage-related vectors and broadcasts them to the different controllable units.

In this work, we propose a fully distributed optimization algorithm to perform real-time voltage control of LV networks. The proposed distributed control minimizes the communication burden and ensures data privacy. Each electrical node is responsible for computing its power setpoints. We leverage the convergence properties of consensus-based ADMM and its iterative procedure to pursue the solution of an optimal power flow. The contributions of this work are the following:

- No need for a central coordinator. Small optimization problems are solved at each electrical node using local estimations for power and measured voltage magnitudes.
- A linear version of the branch flow model is implemented using an estimation of the line currents. Unlike common linearization methods, the losses are not neglected; they are evaluated for each line and each iteration. This method allows the use of a convex model which does not need the usual loss minimization term for the convex relaxation to be exact.

Section II describes the optimization problem formulation and how the computation is distributed, Section III introduces the time-varying problem and the case study, Section IV presents the results, which are then compared to the solution of a centralized approach to our problem, and Section V concludes.

II. Problem formulation and decomposition

A. Centralized model

Residential LV networks, except for some large towns, have a radial topology [18]. The *DistFlow* model is particularly well adapted to radial networks [19]. It is employed in this work and described below:

$$\min_{p,q} \sum_j f_j(p_j, q_j) \tag{1}$$

subject to

Branch Flow Constraints

$$p_j - p_{cons,j} = \sum_{(jk)\in\mathcal{E}} P_{jk} - \sum_{(ij)\in\mathcal{E}} (P_{ij} - r_j l_j)\ \forall j, \tag{1a}$$

$$q_j - q_{cons,j} = \sum_{(jk)\in\mathcal{E}} Q_{jk} - \sum_{(ij)\in\mathcal{E}} (Q_{ij} - x_j l_j)\ \forall j, \tag{1b}$$

$$v_j = v_i - 2\left(r_j P_{ij} + x_j Q_{ij}\right) + \left(r_j^2 + x_j^2\right) l_j,\ \forall (i,j) \in \mathcal{E}, \tag{1c}$$

$$l_j = \frac{P_{ij}^2 + Q_{ij}^2}{v_i},\ \forall (i,j) \in \mathcal{E}, \tag{1d}$$

Generator Constraints

$$p_j, q_j \in \mathcal{S}_j\ \forall j, \tag{1e}$$

Network Constraints

$$v_j \in \mathcal{V}\,\forall j, \tag{1f}$$

where (p_j, q_j) are the active and reactive power injected at node j, (P_{ij}, Q_{ij}, l_j) are the active, reactive power and squared current magnitude flowing in the line from i to j at node i, $r_j + jx_j$ the impedance of this line. Variables v_i and v_j are the squared voltage magnitudes of nodes i and j.

The generator constraints describe the physical limitations of the PV inverter. The operating point (p_j, q_j) is in the set $\mathcal{S}_j$ if:

- the net apparent power does not exceed the inverter's rated capacity:
$$p_j^2 + q_j^2 \leq S_{nom,j}^2, \tag{2}$$
- the present maximum power of the PV system limits the active power injection:
$$0 \leq p_j \leq P_{max,j}, \tag{3}$$
- following Belgian technical prescription, reactive power withdrawn or injected by the inverter is limited to:
$$-p_j \leq q_j \leq p_j, \tag{4}$$
$$-S_{nom,j}/3 \leq q_j \leq S_{nom,j}/3. \tag{5}$$

In this work, the focus point is voltage regulation using PV inverters. The network constraints are limited to keeping the squared voltage magnitude within a given range:

$$v_j \in \mathcal{V} \iff 0.95^2 \leq v_j \leq 1.05^2. \tag{6}$$

The objective function f_j measures the PV curtailment and the reactive power regulation for each inverter:

$$f_j(p_j, q_j) = c_p \left(\frac{(P_{max,j} - p_j)}{S_{nom,j}}\right)^2 + c_q \left(\frac{q_j}{S_{nom,j}}\right)^2, \tag{7}$$

with c_p and c_q weight factors for active curtailment and reactive power. We chose $c_p >> c_q$ to primarily avoid active power curtailment. As a secondary objective, c_q is used to prevent large reactive power flows in the network. We did not consider a loss minimization term because this would result in greater active power curtailment.

Due to (1d), the *DistFlow* model is non-convex. This constraint is commonly relaxed by changing the equality constraint to an inequality constraint [19]. However, this modification is only exact when the objective minimizes the power losses in the system. This would imply increased active power curtailment, which is not desired. A cutting planes technique has been investigated to ensure the convergence of the *DistFlow* model without considering power losses in the objective [20]. However, it will make the algorithm slower and is thus inappropriate for real-time control. Another option is to use a linear version of the *DistFlow* model, neglecting power losses. This simplified formulation is inaccurate for LV networks where the losses are significant.

As a result, in this work, we leverage ADMM's iterative process to define a convex version of the *DistFlow* model while still considering power losses in the problem formulation. The decomposition and the formulation of a convex surrogate of the problem are detailed hereafter.

B. Distributed model

We employ the consensus-based ADMM [21] to distribute the problem (1). The decision variables p_j, q_j and the objective function are specific to each node. Constraints (1a),(1b),(1c),(1d) are coupling neighboring nodes.

Active and reactive power flowing in one line are needed to compute the power balance constraints (1a) and (1b) at both ends of the line. Squared voltage magnitudes are also shared, each node (j) needs the squared voltage level of its ancestor (v_a) to compute its own (v) in (1c).

The network is radial, it is represented using a directed graph rooted at the MV-LV connection node (slack node). Each of the other nodes ($j \neq 0$) has a unique ancestor ($\mathcal{A}_j = \{a : a \to j\}$) and any number of children ($\mathcal{C}_j = \{n : j \to n\}$). This formulation is used to have consistency in the variables. A positive power flows from the ancestor to the children and all line power variables are considered on the side of the ancestor node.

In the consensus-based ADMM, coupled variables are turned into local copies, and an additional consensus constraint imposes the equality of local copies to a shared consensus variable. The consensus constraint is dualized. The consensus variables are computed as the mean of the local copies. As a result, a communication network matching the electrical network must be created to share corresponding local variables between neighboring nodes.

The ADMM iterative procedure is implemented as follows:

- **Step 1:** Solve the subproblem at each node j,
- **Step 2:** Exchange local copies with the neighbors of j,
- **Step 3:** Update the consensus variables.
- **Step 4:** Update scaled dual variables corresponding to the consensus variables using dual ascent.

These four steps are repeated until convergence of primal and dual variables, which ensures the optimality of the solution.

a) Step 1: The subproblem solved at each node j is:

$$\min_{p,q} f_j(p_j, q_j) + N_j(\mathbf{P^j}, \mathbf{Q^j}, \mathbf{v^j}) + M_j(v^j, v_a^j) \tag{8}$$

subject to

Branch Flow Constraints

$$p_j - p_{cons,j} = \sum_{n \in \mathcal{C}_j} P^j_{c_n} - \left(P^j_a - r_j l_j\right), \tag{8a}$$

$$q_j - q_{cons,j} = \sum_{c \in \mathcal{C}_j} Q^j_{c_n} - \left(Q^j_a - x_j l_j\right), \tag{8b}$$

$$v^j = v^j_a - 2\left(r_j P^j_a + x_j Q^j_a\right) + \left(r_j^2 + x_j^2\right) l_j, \tag{8c}$$

Generator constraints

$$p_j, q_j \in \mathcal{S}_j, \tag{8d}$$

Network Constraints

$$v^j \in \mathcal{V}. \tag{8e}$$

The penalty term N_j comes from the augmented Lagrangian is in its scaled form [21]:

$$\begin{aligned} N_j(\cdot) =& \frac{\rho}{2}(||P^j_a - \bar{P}^j_a + \gamma^j_a||_2^2 + ||Q^j_a - \bar{Q}^j_a + \delta^j_a||_2^2 \\ &+ ||v^j_a - \bar{v}^j_a + \alpha^j_a||_2^2 + ||v^j - \bar{v}^j + \alpha^j||_2^2 \\ &+ \sum_{n \in \mathcal{C}_j} (||P^j_{c_n} - \bar{P}^j_{c_n} + \gamma^j_{c_n}||_2^2 + ||Q^j_{c_n} - \bar{Q}^j_{c_n} + \delta^j_{c_n}||_2^2)), \end{aligned} \tag{9}$$

with the penalty parameter or update step (ρ), initialized at 1 and updated using a heuristic described in [21].

The last term M_j is a second penalty term for voltage deviation compared to the measured value:

$$M_j(v^j, v^j_a) = c_v((v^j - V^{j^2}_{meas})^2 + (v^j_a - V^{a^2}_{meas})^2). \tag{10}$$

This aims to keep the local copies of the squared voltage magnitude variables close to the measured values. In distribution network, the MV-LV connection node sets the reference voltage for the system, and the voltage values at other nodes are derived from this reference and the power flow in the lines. The outer nodes thus rely on information from ancestors to determine their own voltage in the ADMM algorithm. Due to the distributed and iterative nature of ADMM, this information takes some time to propagate through the network, resulting in underestimation of voltage values and lasting overvoltages.

Adding this term with a weight factor $c_v > c_q$ speeds up the convergence to solutions that satisfy Kirchhoff's laws, even though this leads to suboptimal operation during convergence. This term ensures faster voltage regulation while optimal operation is still reached when the algorithm has converged (local visions and measurements are equal).

With respect to (1), a superscript j represents a local copy of a variable considered at node j, and variables with subscript a and c are related to the ancestor and the successors of the current node in the directed graph of the network, respectively.

Constraint (1d) is removed to convexify the problem. In (8), the line currents are used nonetheless. They are considered as parameters updated at each iteration of the procedure using:

$$l_j = (\bar{P}_a^{j^2} + \bar{Q}_a^{j^2})/\bar{v}_a^{j^2} \tag{11}$$

b) Step 2: The communication graph described in Fig. 1 shows the variables to be exchanged after each node has solved its subproblem.

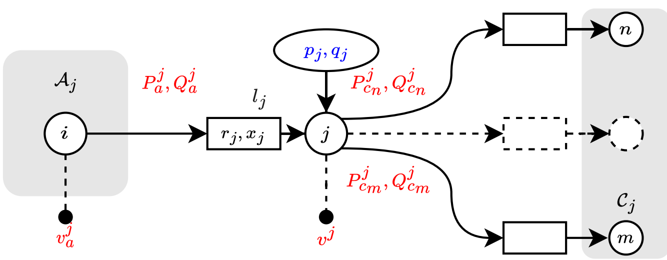

Fig. 1. Communication graph for node j.

c) Step 3: The consensus variables are updated by computing the average value of all the local copies:

$$\begin{aligned}
\bar{v}^j =& (v^j + \textstyle\sum_{n\in\mathcal{C}_j} v_a^{c_n})/(|\mathcal{C}_j|+1), && \text{(12a)}\\
\bar{P}_a^j =& (P_a^j + P_{c_j}^i)/2, \ i \in \mathcal{A}_j && \text{(12b)}\\
\bar{Q}_a^j =& (Q_a^j + Q_{c_j}^i)/2, \ i \in \mathcal{A}_j && \text{(12c)}\\
\bar{P}_{c_n}^j =& (P_{c_n}^j + P_a^n)/2, \ \forall\, n \in \mathcal{C}_j && \text{(12d)}\\
\bar{Q}_{c_n}^j =& (Q_{c_n}^j + Q_a^n)/2, \ \forall\, n \in \mathcal{C}_j. && \text{(12e)}
\end{aligned}$$

Only communication with adjacent buses is used in the algorithm. In order to update $\bar{v}_a$, information from the children nodes of i is needed. This consensus variable is thus only updated in node i with data from all its children, then shared.

d) Step 4: The scaled dual variables are updated with a gradient ascend method:

$$\begin{aligned}
\alpha^j =& \alpha^j + v^j - \bar{v}^j, && \text{(13a)}\\
\alpha_a^j =& \alpha_a^j + v_a^j - \bar{v}_a^j, && \text{(13b)}\\
\gamma_{c_n}^j =& \gamma_{c_n}^j + P_{c_n}^j - \bar{P}_{c_n}^j, \ \forall n \in \mathcal{C}_j && \text{(13c)}\\
\gamma_a^j =& \gamma_a^j + P_a^j - \bar{P}_a^j, && \text{(13d)}\\
\delta_{c_n}^j =& \delta_{c_n}^j + Q_{c_n}^j - \bar{Q}_{c_n}^j, \ \forall n \in \mathcal{C}_j && \text{(13e)}\\
\delta_a^j =& \delta_a^j + Q_a^j - \bar{Q}_a^j. && \text{(13f)}
\end{aligned}$$

III. Case study

A. Network description

We use a Dickert benchmark LV network as described in [18], which is available in Pandapower [22]. The parameters for the Dickert network are *long* range feeders, *multiple customers*, *cables* as line type, and the case type is *average* with a total of 122 buses. Initial electrical loads are maintained, and static generators are added to represent PV systems. The PV systems are randomly distributed among the system's buses, while the number of installations is set to 109, corresponding to a penetration rate of 90%. The rated size of the inverters is

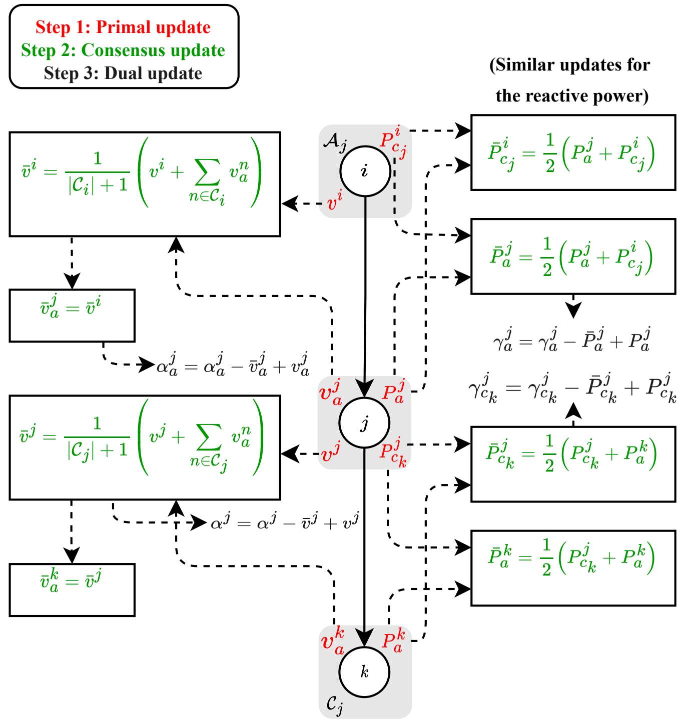

Fig. 2. Consensus and dual updates for node j

.

selected among three different sizes (8, 9 or 10 kVA). Time-domain values for load consumption and PV production with a minute resolution come from [23]. We derived 40 load profiles and 40 PV production profiles collected over several days to simulate active and reactive load consumption patterns and PV system orientations. The data are linearly interpolated to create profiles with second resolution. They are attributed to electrical loads and generators to run the simulations.

B. Scenario

The simulations are run for one day, from sunrise to sunset. Considering the very low computation time and the direct communication between buses, the frequency of the ADMM algorithm is estimated to be 10 Hz. Every 0.1 second, the inverters receive new setpoints. Then, voltage measurements are taken and fed back in eq. (8). Considering the one-second resolution for PV and load data, ADMM has 10 iteration to approach convergence before the state of the system is modified. Each second, after system modification, the algorithm benefits from previous operation points as a warm start. Operation points stay similar and dual variables for the problem are already close to convergence. Perfect communication and synchronicity between neighboring inverters is considered for these simulations.

IV. Results

Figure 3 compares the performance of the centralized model and the distributed model. The voltage magnitude at one problematic bus is shown in the top-left figure. We compare

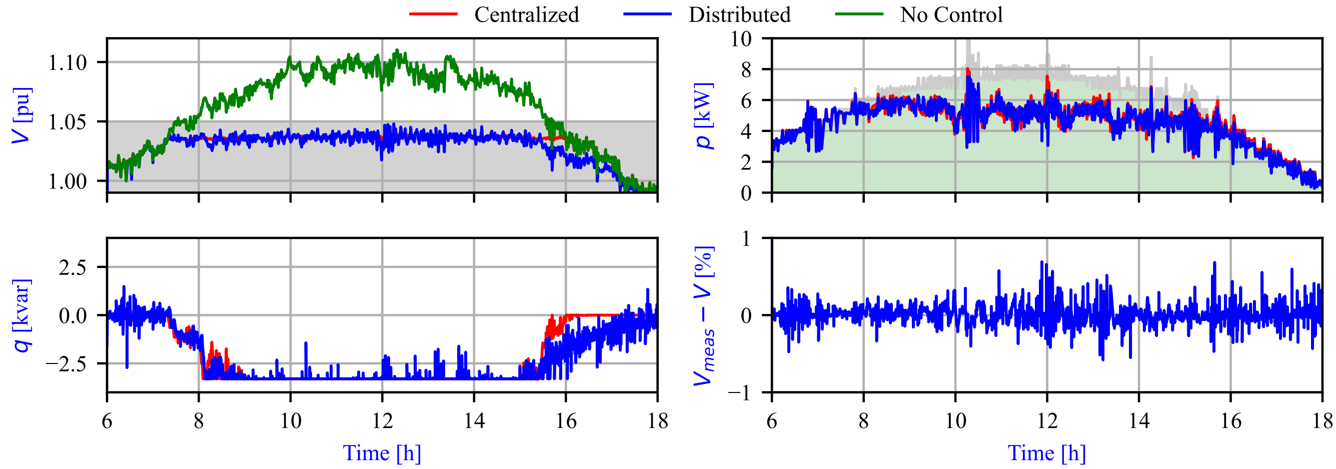

Fig. 3. Results for one specific bus equipped with a PV inverter.

three different simulations. The first two use centralized and distributed models to compute power setpoints. In the third one, no control action is taken (reactive power set to zero and no active power curtailment). The voltage level in the latter case exceeds the 1.05 pu threshold, whereas it does not in the other two cases. Even if the local voltage measurements are not outside boundaries, the distributed algorithm limits the active power to avoid overvoltages in other buses. It can achieve the same results as a centralized model without needing a coordinator with complete observability of the system state. However, the magnitude of the voltage in our model may differ from the network's actual voltage (resulting from the solution of a power flow using the power setpoints computed with the distributed algorithm), as explained before.

The bottom right plot displays the differences between the actual voltage and the voltage perceived by the distributed agents. Finally, we contrast the computed power setpoints for the centralized and distributed algorithms. It is noticeable that the distributed model accurately follows the optimal power setpoints computed with the centralized model.

In Fig. 4, we compare the energy curtailed (integral of the total active power curtailed over a specified period) for three control algorithms. While the centralized and distributed models have already been detailed, we compare the latter two with a decentralized algorithm. The decentralized algorithm follows a rule inspired by Belgium's standard for solar inverters. The inverter is disconnected if:

- the bus voltage goes above 1.1 pu: $v(t) > 1.1$ pu,
- the mean value of the bus voltage for the past 10 minutes is above 1.05 pu: $\int_{t=0}^{T=10min} v(t)dt > 1.05$ pu.

The inverter is reconnected if the voltage level stayed below 1.05 pu for at least 60 seconds. This protective control prevents large overvoltages, but it results in significantly higher energy curtailment compared to the centralized and distributed algorithms. The distributed algorithm performs very well, and yields energy curtailment similar to that of the centralized algorithm.

The control algorithms are compared in terms of overvoltages in Fig. 5 (except the centralized method since it avoids overvoltage). As can be seen, compared to the scenario with no control, the distributed algorithm limits the number of voltage violations and the maximum overvoltage.

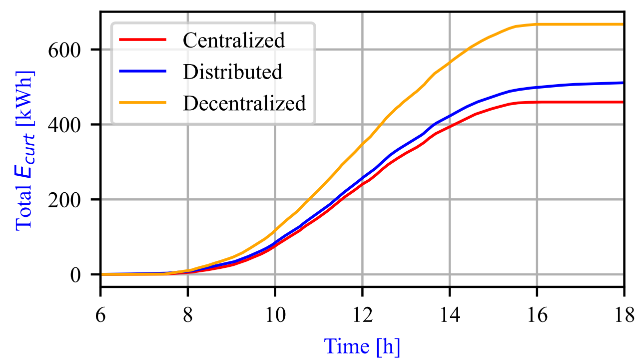

Fig. 4. Energy curtailed for the three control algorithms.

Table I shows the comparative results for the four simulations. The centralized optimizer shows the ideal results, with minimal energy curtailment and no voltage limit violation. The results for the proposed distributed method are relatively close to ideal, with greatly reduced communication needs. The decentralized controllers, which are similar to the methods currently implemented, shows relatively good voltage regulation, at the expense of very large power curtailment.

V. Conclusion

Using ADMM and a direct communication graph between adjacent inverters of a active distribution network, the proposed method can attain similar results as an optimal centralized controller. It uses fast and local control to reach the global optimum for the network. We used a *DistFlow* model decomposed node by node. Using our algorithm's iterative property, we avoided one limitation for this model's exact relaxation. The global optimum can be reached without minimizing the network losses in the model objective thanks to the iterative evaluation of the squared currents in

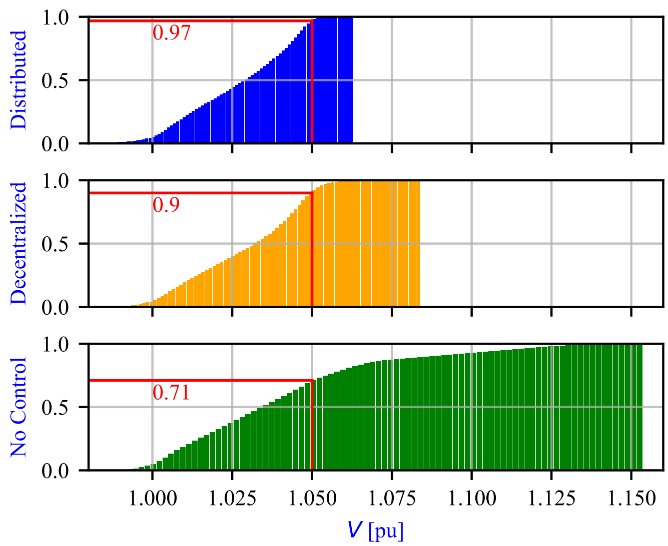

Fig. 5. Cumulative distribution functions of voltages for all nodes in three simulations.

TABLE I
RESULTS FOR THE COMPLETE SIMULATIONS.

	Control algorithm[a]			
	No Ctrl	***Dec. Ctrl***	***ADMM***	***Cent. Op.***
Energy produced	5009kWh	4342kWh	4498kWh	4549kWh
Energy curtailed	0 kWh	697 kWh	511 kWh	460 kWh
Energy lost	212 kWh	123 kWh	186 kWh	191 kWh
Production peak	697 kW	579 kW	591 kW	601 kW
Consumption	679 kWh			
Reactive control	0 kvarh	0 kvarh	1129kvarh	1031kvarh
Max. voltage	1.15 pu	1.08 pu	1.06 pu	1.05 pu
% of overvoltages	29	10	3	0

the lines. The core principle of this method only relies on installed inverter capacity. No additional devices are needed to support the network using this method, only a change in the operation of the inverters using communication with direct neighbors. For instance, this could be achieved using power line communication.

Future work may include the analysis of imperfect communication with varying delays or inexactness in the information communicated, a fully parallel implementation with distributed computation running at each inverter, an analysis of the effect of desynchronization of the ADMM procedure on adjacent nodes, and the inclusion of other network constraints and control devices.

REFERENCES

[1] V. Sharma, S. M. Aziz, M. H. Haque, and T. Kauschke, "Effects of high solar photovoltaic penetration on distribution feeders and the economic impact," *Renewable and Sustainable Energy Reviews*, vol. 131, p. 110021, 2020.

[2] M. Thomson and D. G. Infield, "Network power-flow analysis for a high penetration of distributed generation," *IEEE Transactions on Power Systems*, vol. 22, no. 3, pp. 1157–1162, 2007.

[3] S.-E. Razavi, E. Rahimi, M. S. Javadi, A. E. Nezhad, M. Lotfi, M. Shafie-khah, and J. P. Catalão, "Impact of distributed generation on protection and voltage regulation of distribution systems: A review," *Renewable and Sustainable Energy Reviews*, vol. 105, pp. 157–167, 2019.

[4] J. Seuss, M. J. Reno, R. J. Broderick, and S. Grijalva, "Improving distribution network PV hosting capacity via smart inverter reactive power support," in *2015 IEEE Power & Energy Society General Meeting*. IEEE, 2015, pp. 1–5.

[5] H. Ji, C. Wang, P. Li, J. Zhao, G. Song, F. Ding, and J. Wu, "A centralized-based method to determine the local voltage control strategies of distributed generator operation in active distribution networks," *Applied Energy*, vol. 228, pp. 2024–2036, 2018.

[6] X. Sun, J. Qiu, and J. Zhao, "Optimal local Volt/Var control for photovoltaic inverters in active distribution networks," *IEEE Transactions on Power Systems*, vol. 36, no. 6, pp. 5756–5766, 2021.

[7] K. E. Antoniadou-Plytaria, I. N. Kouveliotis-Lysikatos, P. S. Georgilakis, and N. D. Hatziargyriou, "Distributed and decentralized voltage control of smart distribution networks: Models, methods, and future research," *IEEE Transactions on Smart Grid*, vol. 8, no. 6, pp. 2999–3008, 2017.

[8] H. S. Bidgoli and T. Van Cutsem, "Combined local and centralized voltage control in active distribution networks," *IEEE Transactions on Power Systems*, vol. 33, no. 2, pp. 1374–1384, 2017.

[9] R. Gupta, F. Sossan, and M. Paolone, "Grid-aware distributed model predictive control of heterogeneous resources in a distribution network: Theory and experimental validation," *IEEE Transactions on Energy Conversion*, vol. 36, no. 2, pp. 1392–1402, 2020.

[10] S. Karagiannopoulos, P. Aristidou, and G. Hug, "Data-driven local control design for active distribution grids using off-line optimal power flow and machine learning techniques," *IEEE Transactions on Smart Grid*, vol. 10, no. 6, pp. 6461–6471, 2019.

[11] S. Ghosh, S. Rahman, and M. Pipattanasomporn, "Distribution voltage regulation through active power curtailment with PV inverters and solar generation forecasts," *IEEE Transactions on Sustainable Energy*, vol. 8, no. 1, pp. 13–22, 2016.

[12] J. Li, Z. Xu, J. Zhao, and C. Zhang, "Distributed online voltage control in active distribution networks considering PV curtailment," *IEEE Transactions on Industrial Informatics*, vol. 15, no. 10, pp. 5519–5530, 2019.

[13] S. Bolognani, R. Carli, G. Cavraro, and S. Zampieri, "Distributed reactive power feedback control for voltage regulation and loss minimization," *IEEE Transactions on Automatic Control*, vol. 60, no. 4, pp. 966–981, 2014.

[14] B. Zhang, A. Y. Lam, A. D. Domínguez-García, and D. Tse, "An optimal and distributed method for voltage regulation in power distribution systems," *IEEE Transactions on Power Systems*, vol. 30, no. 4, pp. 1714–1726, 2014.

[15] P. Šulc, S. Backhaus, and M. Chertkov, "Optimal distributed control of reactive power via the alternating direction method of multipliers," *IEEE Transactions on Energy Conversion*, vol. 29, no. 4, pp. 968–977, 2014.

[16] T. Xu and W. Wu, "Accelerated ADMM-based fully distributed inverter-based volt/var control strategy for active distribution networks," *IEEE Transactions on Industrial Informatics*, vol. 16, no. 12, pp. 7532–7543, 2020.

[17] Y. Zhang, M. Hong, E. Dall'Anese, S. V. Dhople, and Z. Xu, "Distributed controllers seeking AC optimal power flow solutions using ADMM," *IEEE Transactions on Smart Grid*, vol. 9, no. 5, pp. 4525–4537, 2017.

[18] J. Dickert, M. Domagk, and P. Schegner, "Benchmark low voltage distribution networks based on cluster analysis of actual grid properties," in *2013 IEEE Grenoble Powertech Conference*. IEEE, 2013, pp. 1–6.

[19] M. Farivar and S. H. Low, "Branch flow model: Relaxations and convexification—Part I," *IEEE Transactions on Power Systems*, vol. 28, no. 3, pp. 2554–2564, 2013.

[20] H. Gao, J. Liu, L. Wang, and Y. Liu, "Cutting planes based relaxed optimal power flow in active distribution systems," *Electric Power Systems Research*, vol. 143, pp. 272–280, 2017.

[21] S. Boyd, N. Parikh, E. Chu, B. Peleato, J. Eckstein *et al.*, "Distributed optimization and statistical learning via the alternating direction method of multipliers," *Foundations and Trends® in Machine learning*, vol. 3, no. 1, pp. 1–122, 2011.

[22] L. Thurner, A. Scheidler, F. Schäfer, J.-H. Menke, J. Dollichon, F. Meier, S. Meinecke, and M. Braun, "pandapower—an open-source python tool for convenient modeling, analysis, and optimization of electric power systems," *IEEE Transactions on Power Systems*, vol. 33, no. 6, pp. 6510–6521, 2018.

[23] Open power system data. 2020. data package household data. version 2020-04-15. [Online]. Available: https://data.open-power-system-data.org/household_data/2020-04-15/